View metadata, citation and similar papers at core.ac.uk

brought to you by CORE

provided by Loughborough University Institutional Repository

This item was submitted to Loughborough's Institutional Repository (https://dspace.lboro.ac.uk/) by the author and is made available under the following Creative Commons Licence conditions.

COMMONS DEED

Attribution-NonCommercial-NoDerivs 2.5

You are free:

- to copy, distribute, display, and perform the work

Under the following conditions:

Attribution. You must attribute the work in the manner specified by the author or licensor.

Noncommercial. You may not use this work for commercial purposes.

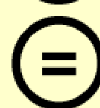

No Derivative Works. You may not alter, transform, or build upon this work.

- For any reuse or distribution, you must make clear to others the license terms of this work.
- Any of these conditions can be waived if you get permission from the copyright holder.

Your fair use and other rights are in no way affected by the above.

This is a human-readable summary of the Legal Code (the full license).

Disclaimer

For the full text of this licence, please go to: http://creativecommons.org/licenses/by-nc-nd/2.5/

Formation of Sn Dendrites and SnAg Eutectics in a SnAgCu Solder

Jicheng Gong[a], Changqing Liu[b], Paul P. Conway[b], Vadim V. Silberschmidt[b]
[a]Department of Materials, University of Oxford, Parks Road, Oxford, OX1 3PH, UK
[b]Wolfson School of Mechanical and Manufacturing Engineering
Loughborough University, Loughborough, LE11 3TU, UK

The formation behaviour of grains and their components, including Sn dendrites, Cu_6Sn_5 and Ag_3Sn intermetallic compounds (IMCs), in a SnAgCu alloy is investigated in an experiment, capable to obtain the solid reactants directly from the liquid solder during the liquid-to-solid phase transformation. The results show that Cu_6Sn_5 IMCs are formed first in a grain; then large Sn dendrites; fibre-like Ag_3Sn IMCs are formed ahead of the β-Sn matrix in the coupling process generating eutectics.

Key words: soldering; eutectic solidification; dendrite growth; intermetallics

In the eutectic SnAgCu alloy, one of the most promising Pb-free candidates for solder interconnections in electronic packages, the main components are Ag_3Sn, Cu_6Sn_5 IMCs and β-Sn. Under equilibrium solidification, Ag_3Sn and Cu_6Sn_5 IMCs are formed in the β-Sn matrix, leading to a uniform eutectic microstructure. However, this alloy system usually deviates from the eutectic transformation in manufacturing processes, e.g., due to a relatively high cooling rate. In most cases, large amounts of soft Sn

dendrites are generated in a grain [1-4]. Sometimes, large brittle Ag_3Sn plates, which can stretch across the entire joint, are found [5]. The formation behaviour of these microstructural components is important, since the size of solder joints has been miniaturized to the same scale as that of grains: a joint contains only one or a few grains [6-9]. Considering the relatively large size and the anisotropic characteristics, the character of a grain plays an important role in a small joint's performance. Recent works have demonstrated this influence on both the mechanical [10,11] and electrical behaviour [12] of some Sn-based solders. To optimize the microstructure of a solder joint with a few grains, better understanding of the formation behaviour of main phases and IMCs in solder materials at the grain or sub-grain level is required. This paper investigates the microstructure that is formed in SnAgCu solder bumps during solidification. Basic components, including β-Sn dendrites, Ag_3Sn, Cu_6Sn_5 IMCs in eutectics and the β-Sn matrix, were studied to present a whole process of formation of a SnAgCu grain.

Due to the absence of solid-state phase transformations in the SnAgCu eutectic alloy from the melting point to room temperature, its microstructure is mainly determined by the liquid-to-solid transformation. The experiments were specially designed to obtain the solid reactants out of the liquid solder during reflow. Details of the set-up were present in [13]. In experiments, a circle printed circuit board (PCB) specimen with Cu pads (the solder material is placed on these pads) on the edge, is fixed to a spindle placed in an oven. The distance between the centre of PCB specimen and a bump is 5 mm. The temperature of solder bumps of the specimen is continuously monitored during reflow. When the solder bump reaches a specific temperature, spinning of the spindle is triggered with the rotation rate of 10000 rpm.. Still-liquid parts of the solder

are removed from the Cu pads due to the centrifugal force, leaving there only solid reactants. The rotation rate is chose based on the criteria that it is high enough to remove quickly the remaining liquid from solid reactant, while it still causes no mechanical deformation on the solid reactants. By a series of these spinning tests at different stages of solidification, the whole process of formation of solid reactants out of the liquid phase can be presented. The solder material used in this study is a commercial Sn3.8Ag0.7Cu paste, containing 13% flux by weight. Fig. 1a presents the pre-designed temperature profiles for the tests; Fig. 1b demonstrates an enlarged portion of the curve in Fig. 1a for the cooling stage.

When solidification occurs in a solder bump, the temperature increases at the cooling stage, as shown in Fig. 1b, due to the released heat. The change in temperature corresponds to the whole process of solidification: the moment that the temperature increases indicates its start; the drop in temperature shows that the transformation is close to the end. A spinning test is conducted at the beginning of the heat release (Point A in Fig. 1b); the respective image is given in Fig. 2a. It shows that there is an oxidized layer on the surface of the bump, and a part of this layer is broken. Under this oxidized layer, a large amount of Sn dendrites is distributed inside the bump, indicating a semi-solidified stage of the process. Obviously, the space between dendrites before spinning is filled with the liquid solder, which is removed from the bump through the broken oxidized layer. The results show that Sn dendrites are formed earlier that the Sn matrix in eutectics: once β-Sn is nucleated, it grows quickly, forming large-size dendrites. Considering the fact that the lattice of a Sn dendrite is consistent with that of the β-Sn matrix of adjacent eutectics [1, 6], it is suggested that the Sn matrix in SnAgCu eutectics is formed from the existing Sn dendrites, and retains the same lattice

orientation. In this case, the size of Sn grains is predominantly controlled by the formation behaviour of Sn dendrites. Figure 2b shows that the size of an individual Sn dendrite can reach several hundreds micrometers. This phenomenon explains the fact that a SnAgCu grain can have such a large size, and a solder joint contains only a few grains. The consistent lattice of Sn dendrites and the β-Sn matrix means that the orientation of Sn grains is determined by that of the initial dendrites at the nucleation stage. Figure 2c captures some dendrites at such a stage. It shows that some Sn dendrites are nucleated on the oxidized layer. This heterogeneous nucleation requires a lower energy and leads to relatively low undercooling (about 10 K).

To further investigate parameters of Sn dendrites, one of them is selected and focused on (Fig. 2b). The figure demonstrates that the size of the dendrite is large (more than 500 μm) in the longitudinal direction, which is considered as the major growth direction. In this direction, the dendrite can be divided into two parts according to its diameter: the main body of the dendrite and the tip. In the main body, there is a long spine in the centre along the dendrite's major growth direction, the diameter of which is about 50 μm. In the direction normal to the spine, secondary arms grow from the spine. The size of secondary arms varies; the ratio of primary to secondary arms is approx. 3. However, some of them seem to grow in the same direction as seen in Fig. 2b for secondary arms 1 to 11. The spacing between secondary arms is approx. 30 μm. With respect to the tip of the dendrite, its diameter (normal to the major growth direction) reduces gradually and finally ends in a sharp tip as shown in Fig. 2a. An interesting observation is that the tip does not grow straightforward but turns sideward. Looking at the entire bump in Fig. 2a, it is obvious that the front tip is close to the surface of the bump. It is suggested that the growth of the Sn dendrite is limited by the boundary of

the bump. In other words, the morphology of a bump, e.g., its shape and size, can influence the growth behaviour of dendrites. To correlate the growth behaviour and the internal lattice orientation, a slice is lifted out of the tip of a dendrite, as shown in Figs. 2d, e and f, for transmission electron microscopy (TEM) analysis. The diffraction pattern and energy-dispersive X-ray (EDX) analysis on TEM confirms that the investigated structure is a single crystal of β-Sn. The diffraction pattern also shows that the [110] direction is close to the preferable growth orientation of the investigated Sn dendrite.

To study the subsequent phase transformation, a bump is tested at Point B (shown in Fig. 1b), which is close to the end of the temperature increase stage; Fig. 3a presents the solder on the bump. It can be seen that most of the bump has became solid, indicating that the solidification is close to the end. Figure 3b presents a local area of Fig. 3a; it shows that dendrites are extruded from the relatively flat surfaces. These relatively flat surfaces at the bottom of, or between, dendrites are undergoing active growth at this moment. Comparing with the microstructure of a fully solidified solder and considering relative locations of each component, these surfaces reflect the growth behaviour of SnAgCu eutectics; they are the interface between eutectics and the liquid solder. Figure 3c focuses on a local area of these surfaces. It can be seen that the eutectics/liquid interface is not flat at the micro scale. A large amount of micro cusps is spread over it, with their tips extruding towards the liquid. A diffraction pattern with EDX on TEM shows that these needles are Ag_3Sn IMCs. This indicates that Ag_3Sn IMCs are formed ahead of the Sn matrix in the coupling process, generating eutectics. To investigate the growth behaviour of these Ag_3Sn IMCs, a cross-section is prepared on the surface of eutectics as shown in Fig. 4b. It can be seen that Ag_3Sn has fibre morphology in the Sn

matrix, with the longitudinal direction of fibres close to the normal to the solid/liquid interface. The axial direction is the preferable growth orientation of these fibres. To characterize these Ag_3Sn fibres, a fully solidified specimen is prepared with deep etching. By removing Sn dendrites and the Sn matrix, Ag_3Sn fibres in eutectics are presented as shown in Fig. 4c. It can be seen that the length of these Ag_3Sn fibres can be more than 100 μm, and that they are orderly distributed: these fibres are orientated nearly in the same direction. To explore the formation behaviour with this regularity, a TEM specimen is prepared on the cross-section in Fig. 4b and presented in Fig. 4d. Diffraction analysis is performed on the TEM specimen. It confirms that an individual Ag_3Sn fiber is a single crystal by achieving the same diffraction pattern at different sites of one fiber. It is also found that all the analyzed Ag_3Sn fibres have a similar lattice orientation. A further analysis shows that the lattice orientation of Ag_3Sn fibres have some relation to that of the β-Sn matrix as demonstrated by diffraction patterns in Figs. 4d, e and f: plane (02-1) and direction [-112] in Ag_3Sn fibres have the same orientation as that of plane (001) and direction [011] in the β-Sn matrix, respectively. The index in Fig. 4g also shows that the axial direction of the preferable growth of Ag_3Sn fibres is close to the one, normal to the plane (02-1).

The same orientation of different Ag_3Sn fibres could result from their nucleation behaviour: the obtained Ag_3Sn/β-Sn lattice pair may have the lowest interfacial energy; Ag_3Sn fibres are nucleated based on the same existing Sn dendrites or matrix with this interface, resulting in the same lattice orientation. Since Ag_3Sn IMCs are formed ahead of the β-Sn matrix, their growth predominantly determines the movement of the eutectics/liquid interface. When two eutectics/liquid interfaces from different grains meet each other, a grain boundary is formed. Figure 4a captures the formation

behaviour of such grain boundary. At this moment, the formation of the grain is close to the end.

Some Cu_6Sn_5 IMCs are found to form prior to Sn dendrites, having the morphology of long needles. Figures 2a and b present some of these Cu_6Sn_5 IMCs. During reflow, the Cu substrate dissolves into the liquid solder. According to the concept of the local nominal composition (LNC) [14], the ratio of Ag to Sn composition is constant in the bump. The Cu composition is higher when the local site is closer to the substrate. In some locations, e.g. near the substrate, the LNC could be in the Cu_6Sn_5 region in the phase diagram as shown in [9]. In this case, Cu_6Sn_5 IMCs are the primary phase during solidification. Since these IMCs are formed earlier, sometimes they are encircled by Sn dendrites.

In summary, this paper studies the formation behaviour of a grain in SnAgCu solder bumps during solidification. The results show that: Cu_6Sn_5 IMCs are formed first among the investigated reactants. They have the cusps-like morphology, and can be embedded in Sn dendrites. Sn dendrites are generated earlier than the Sn matrix in SnAgCu eutectic. Their lattice determines the orientation of the final Sn-phase in the grain. The size of a Sn dendrite can reach hundreds of micro-metres, which predominantly determines the large size of a SnAgCu grain. Eutectics are formed after, and from, Sn dendrites. In eutectics, Ag_3Sn IMCs have morphology of long fibres. They are formed ahead of the Sn matrix in the coupling process to generate eutectics. In addition, Ag_3Sn fibres in eutectics have the same crystal orientation; their lattice is coupled with that of the Sn matrix.

Acknowledgements

The work is financially supported by the Engineering and Physical Sciences Research Council's Innovative Manufacturing and Construction Research Centre at Loughborough University, UK under GR/R64483/01P.

References

[1] A. LaLonde, D. Emelander, J. Jeannette, C. Larson, W. Rietz, D. Swenson, D.W. Henderson, J. Electron. Mater. 33 (2004) 1545.

[2] R.H. Mathiesen, L. Arnberg, F. Mo, T. Weitkamp, A. Snigirev, Phys. Rev. Lett. 83 (1999) 5062.

[3] B. Li, H.D. Brody, A. Kazimirov, Phys. Rev. E. 70 (2004) 062602.

[4] R. Kinyanjui, L.P. Lehman, L. Zavalij, E. Cotts, J. Mater. Res. 20 (2005) 2914.

[5] K. Zeng, K.N. Tu, Mat. Sci. Eng. R 38 (2002) 55.

[6] D.W. Henderson, J.J. Woods, T.A. Gosselin, J. Bartelo, J. Mater. Res. 19 (2004) 1608.

[7] A.U. Telang, T.R. Bieler, S. Choi, K.N. Subranmanian, J. Mater. Res. 17 (2002) 2294.

[8] A.U. Telang, T.R. Bieler, Scripta. Mater. 52 (2005) 1027.

[9] T. Mattila, V. Vuorinen, J.K. Kivilahti, J. Mater. Res. 19 (2004) 3214.

[10] M.A. Matin, E.W.C. Coenen, W.P. Vellinga, M.G.D. Geers, Scripta. Mater. 53 (2005) 927.

[11] A.U. Telang, T.R. Bieler, A. Zamiri, F. Pourboghrat, Acta. Mater. 55 (2007) 2265

[12] M. Lu, D. Shih, P. Lauro, C. Goldsmith, D.W. Henderson, Appl. Phys. Lett. 92 (2008) 211909.

[13] J. Gong, C. Liu, P.P. Conway, V.V. Silberschmidt, Acta. Mater. 56 (2008) 56 4291.

[14] K. Rönkä, F. J. J. van Loo, J.K. Kivilahti, Scr. Mater. 37 (1997) 1575.

Figure Captions

Fig. 1 (a) Temperature profiles during reflow. The cooling rate is 30 K/min. (b) Cooling stage of the curve 1 in (a).

Fig. 2 Sn dendrites formed in a Sn3.8Ag0.7Cu solder bump at Point A in Fig. 1b: (a) entire bump; (b) local area; (c) nucleation of Sn dendrites on the inner surface of the oxidized layer. A tip of the β-Sn dendrites: (d) large area; (e) local area; (g) TEM image and diffraction pattern of the tip.

Fig. 3 Sn dendrites and SnAgCu eutectics formed in a Sn3.8Ag0.7Cu solder bump at Point B in Fig. 1b: (a) entire bump; (b) local area of a specimen; (c) surface of eutectics.

Fig. 4 SnAgCu eutectics and grain boundaries formed in a Sn3.8Ag0.7Cu solder bump at Point B in Fig. 1b: (a) large area; (b) cross section on the surface of eutectics; (c) Ag_3Sn fibres formed in SnAgCu eutectics of a fully solidified bump (this specimen is prepared by deep etching); (d) TEM image of a specimen, which is prepared on the cross-section in (b); diffraction pattern on the β-Sn matrix (e), Ag_3Sn IMCs (f) and β-Sn/Ag_3Sn interface (g).

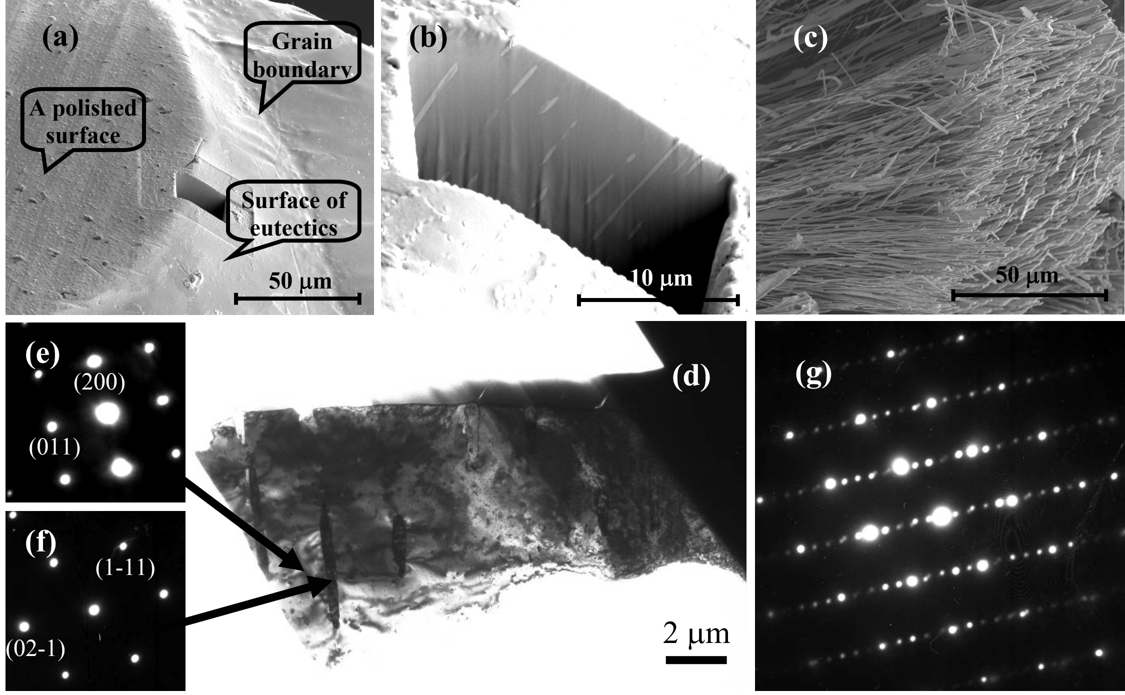
(a)
Grain boundary
A polished surface
Surface of eutectics
50 μm
(b)
10 μm
(c)
50 μm
(e)
(200)
(011)
(f)
(1-11)
(02-1)
(d)
2 μm
(g)

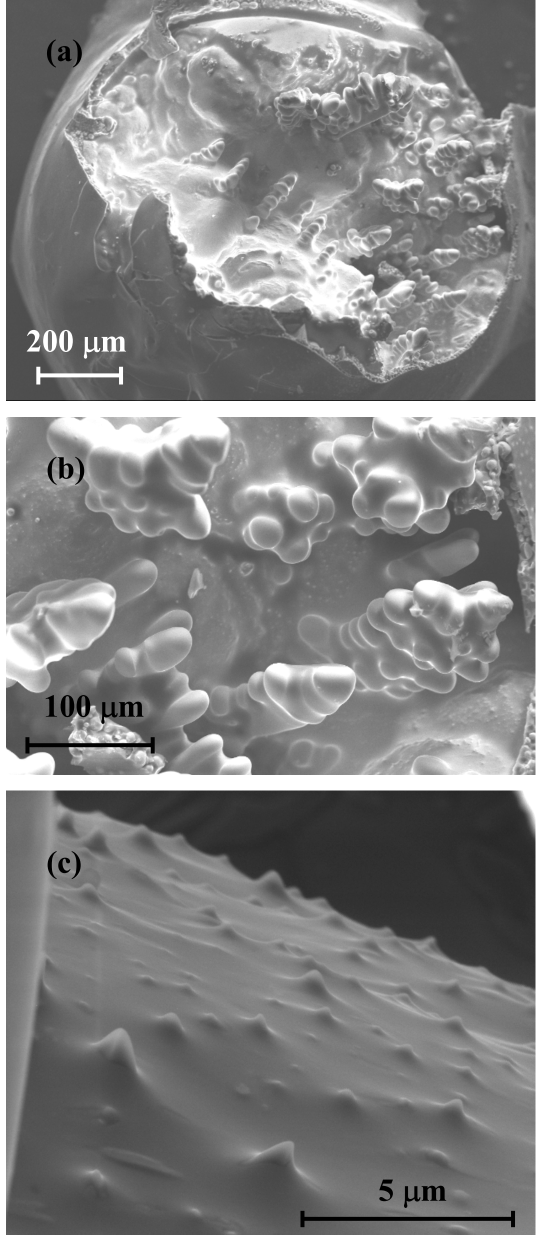
(a)
200 μm
(b)
100 μm
(c)
5 μm

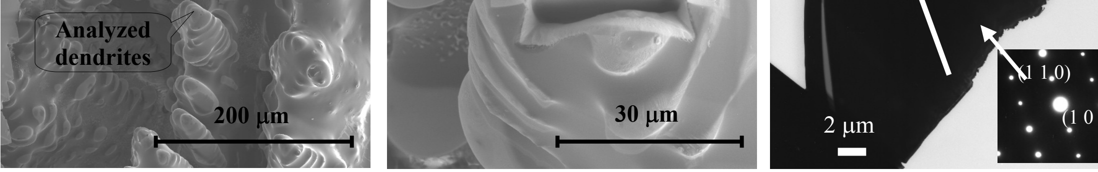

(a)
Oxidized layer
Cu6Sn5
200 μm
(b)
Arm 1
Arm 2
Arm 11
Pine
Cu6Sn5
100 μm
(c)
100 μm
(d)
Analyzed dendrites
200 μm
(e)
30 μm
(f)
[110]
(1 1 0)
(1 0 1)
2 μm

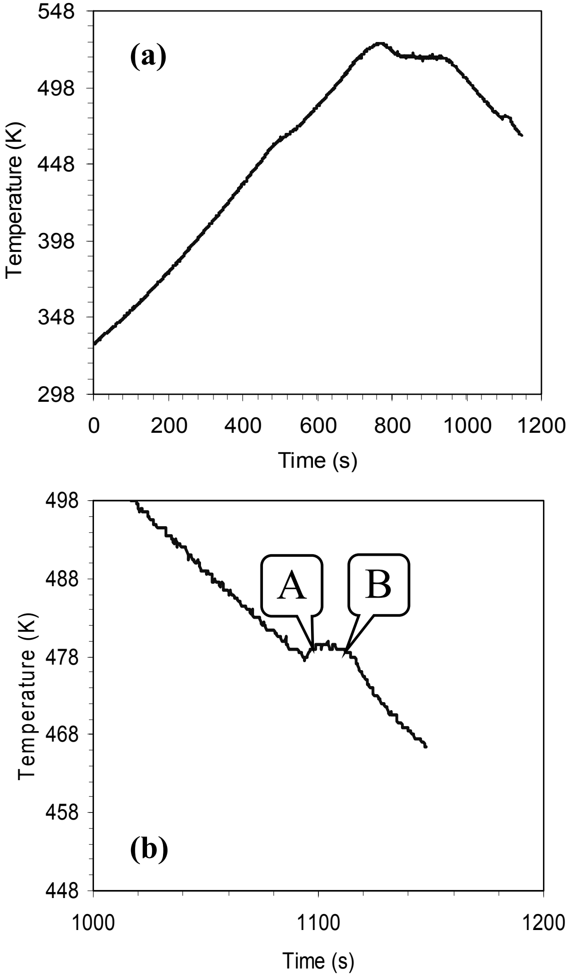

(a)
Temperature (K)
548
498
448
398
348
298
0
200
400
600
800
1000
1200
Time (s)
(b)
Temperature (K)
498
488
478
468
458
448
1000
1100
1200
Time (s)
A
B